

All Patches Matter, More Patches Better: Enhance AI-Generated Image Detection via Panoptic Patch Learning

Zheng Yang^{1*}, Ruoxin Chen^{2*}, Zhiyuan Yan³, Keyue Zhang², Xinghe Fu¹
Shuang Wu², Xiujuan Shu⁴, Taiping Yao², Shouhong Ding², Xi Li^{1†}

¹Zhejiang University

²Youtu Lab, Tencent

³Peking University

⁴Wechat Pay, Tencent

Abstract

The exponential growth of AI-generated images (AIGIs) underscores the urgent need for robust and generalizable detection methods. In this paper, we establish two key principles for AIGI detection through systematic analysis: **(1) All Patches Matter**: Unlike conventional image classification where discriminative features concentrate on object-centric regions, each patch in AIGIs inherently contains synthetic artifacts due to the uniform generation process, suggesting that every patch serves as an important artifact source for detection. **(2) More Patches Better**: Leveraging distributed artifacts across more patches improves detection robustness by capturing complementary forensic evidence and reducing over-reliance on specific patches, thereby enhancing robustness and generalization. However, our counterfactual analysis reveals an undesirable phenomenon: naively trained detectors often exhibit a **Few-Patch Bias**, discriminating between real and synthetic images based on minority patches. We identify **Lazy Learner** as the root cause: detectors preferentially learn conspicuous artifacts in limited patches while neglecting broader artifact distributions. To address this bias, we propose the **Panoptic Patch Learning (PPL)** framework, involving: (1) Random Patch Replacement that randomly substitutes synthetic patches with real counterparts to encourage models to identify artifacts in underutilized regions, encouraging the broader use of more patches; (2) Patch-wise Contrastive Learning that enforces consistent discriminative capability across all patches, ensuring uniform utilization of all patches. Extensive experiments across two different settings on several benchmarks verify the effectiveness of our approach.

1 Introduction

The rapid evolution of generative AI models has precipitated an exponential growth of AI-generated images (AIGIs) in digital ecosystems [5, 11, 12, 10, 25, 43, 24, 39, 38]. This proliferation raises critical concerns regarding information security and content authenticity, highlighting the critical need for AIGI detection methods to distinguish synthetic images from authentic ones. Unlike conventional classification tasks, AIGI detection operates as a "cat-and-mouse game", presenting unique challenges due to: (1) continuous emergence of new generative architectures, and (2) frequent updates to existing models. Consequently, exhaustive training on all synthetic data becomes impractical [20], thus necessitating detectors with strong generalizability.

Although AIGI detection poses additional challenges for models in capturing generalizable features compared to traditional binary classification tasks, AIGIs offer a unique characteristic absent in conventional classification tasks that can be leveraged: **Universal Artifact Distribution**. In the context of AIGIs, discriminative features are not confined to regions with labeled objects; instead,

*: Equal Contribution, †: Corresponding Author

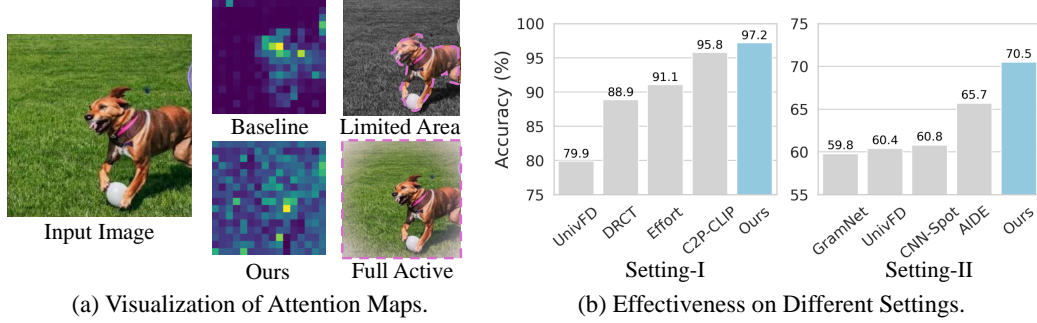


Figure 1: **(a):** The model trained with PPL exhibits a more uniform distribution of attention across nearly all patches, suggesting that PPL facilitates comprehensive artifact detection. **(b):** We compare PPL with other methods under two evaluation settings: Setting-I (GenImage dataset [47]), where the model is trained on images from a specific generative model and tested on synthetic images from various generative models; and Setting-II (Chameleon dataset [36]), where the model is trained on a diverse set of generative models and evaluated on human-imperceptible synthetic images. For further details, see Section 5.

synthetic images present artifacts uniformly across all patches due to the uniform production of generative models.² This finding indicates that every image patch contains synthetic traces, establishing our first principle for AIGI detection: **All Patches Matter**. This principle is also validated by two lines of evidence: (1) Visual analytics [30, 3] confirm pixel-level discriminative patterns in localized regions, revealing artifact presence at patch granularity; (2) recent patch-wise detectors [2, 46] show comparable performance to full-image approaches, proving individual patches’ discriminative capability. Meanwhile, while artifact variations occur across different patches, detectors capable of capturing diverse synthetic artifacts across distributed patches **reduce the over-reliance on specific patches**. This universal artifact capturing enhances cross-generator generalizability by mitigating detectors’ blind spots through distributed artifact aggregation. This leads to our second principle: **More Patches Better**.

However, our counterfactual analysis of existing detectors [20, 16, 28, 8, 1] reveals an unfavorable tendency: **Few-Patch Bias**, involving two empirical observations and a quantitative analysis. The empirical observations: (1) detectors’ attention maps disproportionately focus on very limited image patches, neglecting broader artifact patterns; (2) detectors exhibit severe patch-specific fragility, where masking merely a patch could lead to accuracy degradation by $18.7\% \pm 4.1\%$ on average. Furthermore, by employing the **causal inference tool TDE [33] to quantify each patch’s impact** – calculated as the classification logit difference with and without that patch – we observe that the TDE distribution of naively-trained detectors is characterized by a few patches with high TDE values, while the majority of patches exhibit significantly smaller TDEs. This suggests that **most patches remain underutilized and contribute minimally to the discriminative outcome**, although they also contain generative artifacts. Moreover, when comparing TDE distributions across different detection methods, we find that methods with TDE distributions tending towards a **more uniform distribution exhibit better generalizability**. For instance, DRCT, with more high-TDE patches, performs significantly better than UnivFD. We attribute the Few-Patch Bias to the propensity of detectors as **Lazy Learner** [9, 41, 34, 44, 4, 31, 27, 40, 37]. Specifically, AIGI detectors exhibit curriculum learning behavior: once easily learned synthetic artifacts in certain patches are used to minimize training loss, the presence of these patches reduces the incentive to explore broader regions.

To address this challenge, we argue that **the key lies in following the principle: "all patches matter; more patches better"**, which **ensures that the model does not overly rely on and shortcut to very few regions** for discrimination but instead learns comprehensive and robust features across the entire image. To implement this idea, we propose a practical and effective instance called Panoptic Patch Learning (PPL), which involves: (1) Patch-wise contrastive learning, which aligns the features of different synthetic and real patches, ensuring consistent discriminative capability across all patches. (2) Random patch replacement, which randomly substitutes patches in the synthetic image with real

²This work adheres to the mainstream AIGI detection setting [1, 20, 28, 16, 8, 47, 30] where the entire image is generated by AI models.

counterparts, discourages over-reliance on limited patches and promotes a more uniform utilization of patches. Fig. 1 illustrates the practical function and performance of Panoptic Patch Learning. Our main contributions are threefold:

1. We formally propose the principle "All Patches Matter, More Patches Better" for AIGI detection, demonstrating that broader artifact exploitation can effectively enhance detection.
2. We conduct a detailed patch-wise analysis of AIGI detectors, utilizing the causal inference tool TDE to quantify each patch’s impact, revealing that Few-Patch Bias commonly exists in existing detectors.
3. Based on the "All Patches Matter, More Patches Better" principle, we propose Panoptic Patch Learning. Extensive experimental results validate the effectiveness of our approach.

2 Related Work

Existing AIGI detection methods can be generally categorized into two types: local and global detection methods [28]. We will briefly introduce both of them separately below.

Local AIGI detection methods. Local AIGI detectors utilize the localized information in the image to differentiate AI-generated images from real ones. This approach is based on the assumption that significant differences exist between real and synthetic images in low-level features. These detectors can be categorized into two groups: patch-wise and pixel-wise methods.

Patch-wise methods include: SSP [2] achieves remarkable performance by using only one single simplest patch, while Patchcraft [46] processes the simplest and most complex patches separately by selecting patches with the highest and lowest entropy for detection. [45] employs a patch-based CNN that leverages all patches to avoid selective patch sampling and aggregate patch features from an image. TextureCrop [13] utilizes a sliding window to partition the input image and then ranks and selects the regions of crops that are rich in high-frequency texture information. However, these patch-wise detectors are limited by their over-reliance on a small subset of patches, resulting in insufficient utilization of available patch information.

Pixel-wise methods include: NPR [30], which discriminates between real and AI-generated images by analyzing differences in neighboring pixel relationships; FreqNet [29] and SAFE [15], which use high-frequency information to detect forgeries by focusing on localized feature patterns; and ZED [3], which computes the coding cost of local regions using an entropy-based encoder and identifies AIGIs by detecting gaps in coding costs. However, these pixel-wise detectors are highly sensitive to minor variations in localized pixel relationships, which can limit their robustness in practical applications.

Global AIGI detection methods. Global AIGI detection methods leverage information from the entire image to distinguish AI-generated images from real ones. By analyzing holistic image characteristics, these methods aim to capture global inconsistencies that may not be evident at the local level. CNNSpot [35] simply employs a CNN to detect AIGIs, exhibiting strong performance on seen AIGIs but suffering from poor cross-generator generalizability. UnivFD [20] addresses this limitation by utilizing a CLIP visual encoder as an AIGI feature extractor, significantly improving generalization, FatFormer [16] further improves the CLIP vision encoder’s adaptability by integrating a frequency adapter, C2P-CLIP [28] introduces a novel approach by fine-tuning CLIP with elaborately designed image-text pairs to embed the concepts of "real" and "fake" into the model. DRCT [1] uses a contrastive loss with hard cases to improve UnivFD’s performance, Despite the aforementioned advantages, global information does not encompass detailed artifacts of AIGIs, which severely limits their performance.

3 Motivation

3.1 All Patches Matter, More Patches Better

The principle of **All Patches Matter** is supported by three key findings. (1) **Theory:** Since every patch in synthetic images is inherently synthetic, each patch contains synthetic artifacts. Several localized region-based detection methods [2, 46] demonstrate that trace cues within localized patches

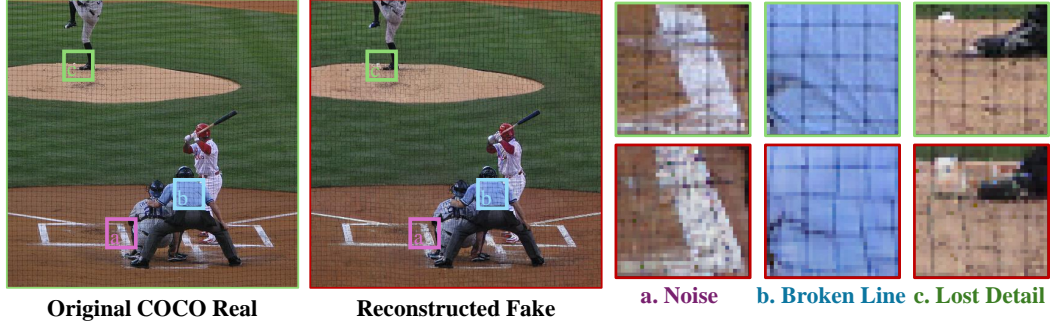


Figure 2: Visualization of different patch-wise artifacts generated by AI models is depicted by comparing real images to their synthetic counterparts reconstructed by diffusion models. We observe various patch-level synthetic traces, such as broken lines, unnatural noise, and lost detail on clear boundaries, indicating a diversity of artifacts among different patches. This observation **supports the need for leveraging more patches to enhance the recognition** capability for different artifacts.

can effectively discriminate between real and synthetic images, achieving substantial performance. This evidence underpins the principle that all patches matter, as each patch carries discriminative artifacts. (2) **Visualization:** Fig. 2 clearly illustrates the distinct artifact patterns present in each patch, demonstrating that every synthetic patch possesses unique and identifiable features that effectively differentiate it from real images. Furthermore, the visual variation in trace cues across different patches highlights and confirms the considerable diversity of artifacts observed. (3) **Experiments:** We evaluated the presence of these artifacts by inputting a randomly selected patch into the detectors, achieving an accuracy of 90% on the SDv1.4 subset of the GenImage dataset. Specifically, we replicated a single patch multiple times to form an image, ensuring that it contains only the features of that patch. The results indicate that detectors can effectively distinguish real from synthetic images even with a single random patch. The results indicate that detectors can effectively distinguish between real and synthetic images even using a single random patch. From visualization and experiments, we recognize that artifacts in each patch are distinct and thus detectors are capable of capturing these artifacts, proving their ability to recognize diverse artifact patterns. This can enhance the generalizability and robustness of the detectors, leading to the principle of **More Patches Better**. However, our observations suggest that existing detectors do not conform to this principle.

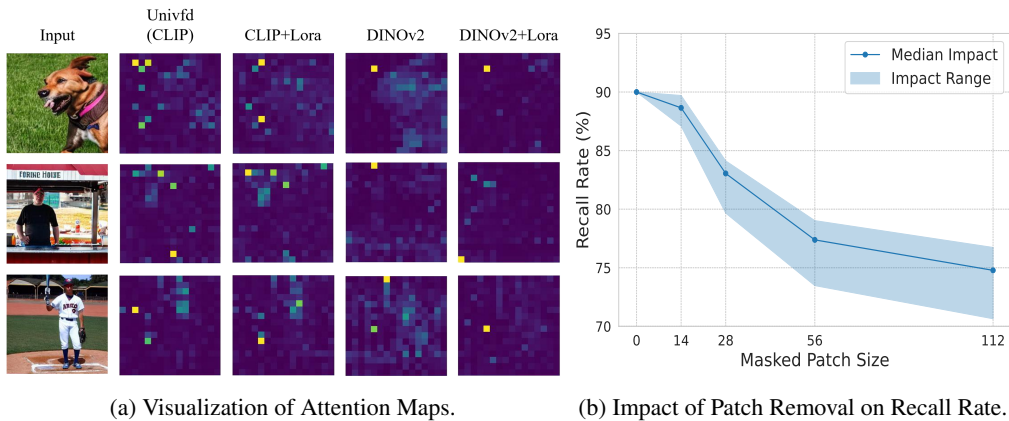


Figure 3: (a) Attention maps reveal the "few patches bias" in naively trained ViT detection models, where attention focuses on a few dominant patches, indicating over-reliance on limited regions. (b) Recall degradation in a naively trained model is shown by occluding single patches of varying sizes. Such models are sensitive to specific patches, causing notable recall drops.

3.2 Few-Patch Bias

Observations. Our empirical observations indicate that existing detectors often overly rely on a limited number of patches. Fig. 3(a) depicts the attention map of naively fine-tuned ViTs, demonstrating that the attention weight concentrates only on a few patches. By changing the ViT backbone and applying Lora fine-tuning, we find a similar observation. To further verify our hypothesis, we mask out the patches of different sizes and observe the degradation of accuracy. Fig. 3(b) visualizes the performance degradation of UnivFD detector concerning the size of the masked patch. We find that masking out a patch can lead to a significant drop in accuracy, and masking out different patches will also result in different drops in accuracy.

Quantitative analysis. Based on the above observation, we utilize the total direct effect (TDE) to evaluate each patch’s impact. To explain TDE, for example, $X \rightarrow Y$ and $Z \rightarrow Y$ indicate that the relationship Y is a combined effect resulting from the content represented by X and Z . The Total Direct Effect (TDE) is calculated as the difference between the effect of Y with X and without X affecting the rest of the parts, namely $Y(X|Z) - Y(\bar{X}|Z)$. We partition an image into $n = m \times m$ patches, and the TDE for each patch (i, j) is defined as follows:

$$TDE := \delta_I - \delta_{I-(i,j)}, \quad \delta := \text{logit}_{syn} - \text{logit}_{real} \quad (1)$$

where I and $I - (i, j)$ represents the original input image and the image with the (i, j) th patch masked, which we implement by setting masked patch to zero. By calculating the TDE for each patch, we can assess its contribution to the classification of a synthetic image.

Fig. 4 visualizes the TDE heatmap for different detectors. From left to right, the cases become progressively easier for the models to detect, as indicated by the increased number of active patches and a more uniform TDE distribution. We reimplemented UnivFD [20], DRCT [1] and Breaking [45] and compare them with our approach, demonstrating that a more effective method tends to discover a greater number of patches. Overall, the visual examples highlight the existing bias towards a limited number of dominant patches with higher TDE. In the methodology section, we will address this issue from a TDE perspective and explore it further with statistical analysis.

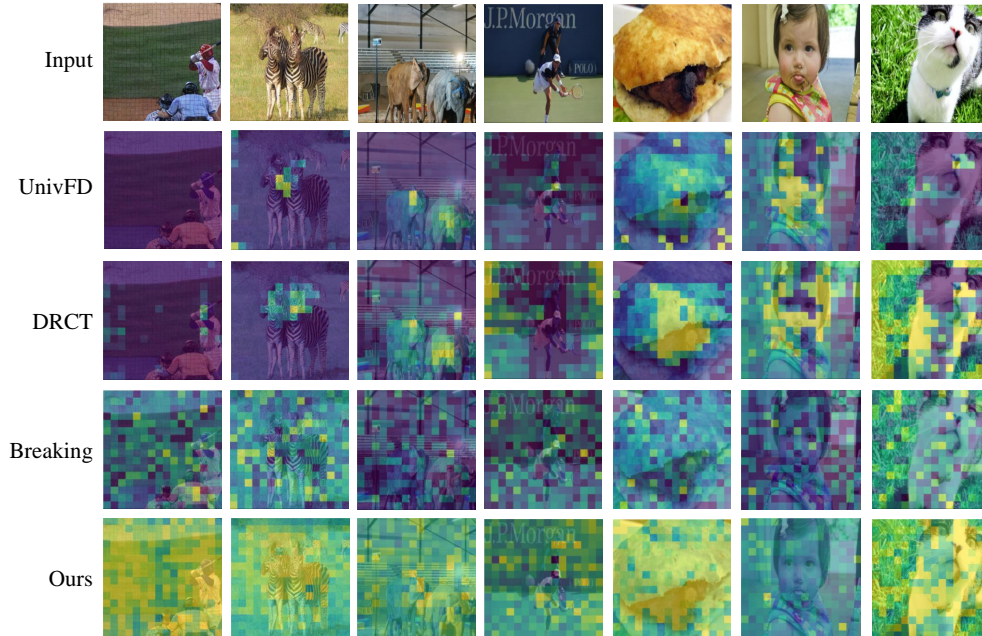


Figure 4: TDE heatmap of existing methods on generated images selected from the DRCT dataset. A broader and **more uniform highlighted region indicates a greater number of patches contributing to determining a fake image**. The results of UnivFD [20], DRCT [1], and Breaking [45] are obtained from our implementation.

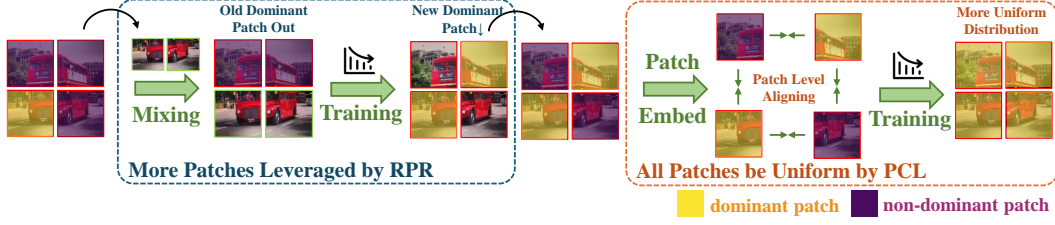


Figure 5: The Panoptic Patch Learning (PPL) framework embodies the principles of **All Patches Matter** and **More Patches Better** through two key components: Random Patch Replacement (RPR) and Patch-wise Contrastive Learning (PCL). During training, the model may rely excessively on the **dominant patch**, neglecting others. RPR mitigates this by randomly replacing dominant patches with real ones, prompting the model to detect artifacts in **non-dominant patches** and thus expanding dominant regions. PCL further promotes balanced patch utilization by aligning embeddings of patches with same labels. Together, RPR and PCL foster comprehensive and uniform patch exploitation.

4 Methodology

Panoptic Patch Learning fulfills the idea of "All Patches Matter" and "More Patches Better" by two key components shown in Fig. 5. Specifically, the data augmentation technique, referred to as Random Patch Replacement (RPR), encourages the model to capture artifacts across a broader range of patches, thereby expanding the coverage of **more patches**. Following this, our learning strategy, Patch-wise Contrastive learning (PCL), ensures that **all patches**, both dominant and non-dominant, are brought closer in the feature space, thereby uniformizing the impact of all patches. Through the combined effect of these two components, we achieve a more comprehensive and balanced representation derived from all patches.

Random Patch Replacement encourages "More Patches Better". Random Patch Replacement (RPR) promotes the principle of "More Patches Better" by encouraging the model to focus on learning from a greater number of detected patches. The RPR process is applied to paired images in which each reconstructed image I' has a corresponding ground truth I . The images are partitioned into $n = m \times m$ patches, and the patch replacement function \mathcal{R} is defined as:

$$\mathcal{R}(P_{i,j}(I')) = \begin{cases} P_{i,j}(I) & \text{if } M_{i,j} = 1, \\ P_{i,j}(I') & \text{otherwise} \end{cases} \quad (2)$$

where $M \in \{0, 1\}^{m \times m}$ is a random sampled binary mask with replacement ratio $r \in [0, 1]$. When dominant patches are replaced with real patches during this process, training the model on these mixed images forces it to learn artifacts from previously non-dominant patches. By dynamically altering the spatial distribution of attended patches through RPR, the model is forced to learn latent representations from previously underutilized regions, thereby reducing over-reliance on dominant local features. As a result, RPR effectively expands the effective region of the model and enhances its overall performance and robustness.

Patch-wise Contrastive Learning emphasizes "All Patches Matter". Patch-wise Contrastive Learning (PCL) operationalizes the principle of "All Patches Matter" by aligning the embedding vectors of different patches, bringing patches with identical labels closer together while distancing those with different labels. We employ contrastive learning to cluster synthetic patches more closely within each batch while maintaining a margin to separate synthetic and real patches. This approach ensures that if an image contains any dominant patch with easily learnable artifacts, the model enhances its performance on the remaining patches, thus leveraging the significance of all patches. Specifically, for each batch, we utilize a margin-based contrastive loss [6] that:

$$\mathcal{L}_{con} = \sum_{i,j,i \neq j} [Y \cdot d^2 + (1 - Y) \cdot \max(0, \alpha - d^2)] \quad (3)$$

where i and j represent the index of patch tokens within a batch. $d = \|\text{Emb}_{\text{pat}}^i - \text{Emb}_{\text{pat}}^j\|_2$ measures the Euclidean distance between the embedded patch tokens. α defines a minimum distance threshold

between negative sample pairs, thereby enhancing the model’s ability to distinguish between similar and dissimilar pairs. $Y = \mathbb{I}[y_{\text{pat}}^i = y_{\text{pat}}^j]$ indicates whether two patches in the pair share identical labels, thus pulling positive patch pairs (with identical patch labels) closer and pushing negative patch pairs (with different patch labels) further. The overall learning objective is a weighted combination of the cross-entropy loss and the patch-wise contrastive loss:

$$\mathcal{L}_{\text{total}} = \lambda \mathcal{L}_{\text{con}} + (1 - \lambda) \mathcal{L}_{\text{ce}} \quad (4)$$

Table 1: Cross-model accuracy (Acc) performance on the GenImage Dataset. All methods are trained on the SDv1.4 subset of the GenImage dataset. We re-implemented Breaking [45] and copied the result of SAFE [15] and Effort [37] from original paper. The rest results can be sourced from [28].

Method	Ref	Midjourney	SDv1.4	SDv1.5	ADM	GLIDE	Wukong	VQDM	BigGAN	mAcc	std
ResNet-50 [7]	CVPR2016	54.9	99.9	99.7	53.5	61.9	98.2	56.6	52.0	72.1	22.6
DeiT-S [32]	ICML2021	55.6	99.9	99.8	49.8	58.1	98.9	56.9	53.5	71.6	23.2
Swin-T [18]	ICCV2021	62.1	99.9	99.8	49.8	67.6	99.1	62.3	57.6	74.8	21.1
CNNSpot [35]	CVPR2020	52.8	96.3	95.9	50.1	39.8	78.6	53.4	46.8	64.2	22.6
Spec [42]	WIFS2019	52.0	99.4	99.2	49.7	49.8	94.8	55.6	49.8	68.8	24.1
F3Net [22]	ECCV2020	50.1	99.9	99.9	49.9	50.0	99.9	49.9	49.9	68.7	25.8
GramNet [17]	CVPR2020	54.2	99.2	99.1	50.3	54.6	98.9	50.8	51.7	69.9	24.2
UnivFD [20]	CVPR2023	93.9	96.4	96.2	71.9	85.4	94.3	81.6	90.5	88.8	8.6
NPR [30]	CVPR2024	81.0	98.2	97.9	76.9	89.8	96.9	84.1	84.2	88.6	8.3
FreqNet [29]	AAAI2024	89.6	98.8	98.6	66.8	86.5	97.3	75.8	81.4	86.8	11.6
FatFormer [16]	CVPR2024	92.7	100.0	99.9	75.9	88.0	99.9	98.8	55.8	88.9	15.7
DRCT [1]	ICML2024	91.5	95.0	94.4	79.4	89.1	94.6	90.0	81.6	89.4	5.9
Effort [37]	ICML2025	82.4	99.8	99.8	78.7	93.3	97.4	91.7	77.6	91.1	11.8
Breaking [45]	NIPS2024	83.9	98.9	93.0	99.1	97.7	85.4	92.7	90.5	92.7	5.8
SAFE [15]	KDD2025	95.3	99.4	99.3	82.1	96.3	98.2	96.3	97.8	95.6	5.6
C2P-CLIP [28]	AAAI2025	88.2	90.9	97.9	96.4	99.0	98.8	96.5	98.7	95.8	4.0
Ours/DINOv2		90.4	98.2	97.7	91.8	96.3	98.0	97.7	96.2	<u>95.9</u>	<u>3.0</u>
Ours/CLIP		94.8	98.5	98.3	94.7	96.1	98.6	98.5	98.0	97.2	1.7

Table 2: Cross-model accuracy (Acc) performance on the DRCT dataset. All methods are trained on the SDv1.4 subset of DRCT. All results of former methods can be sourced from the paper DRCT [1].

Method	SD Variants						Turbo Variants		LCM Variants		ControlNet Variants			DR Variants			mAcc	std
	LDM	SDv1.4	SDv1.5	SDv2	SDXL	SDXL-Refiner	SD-Turbo	SDXL-Turbo	LCM-SDv1.5	LCM-SDXL	SDv1-Ctrl	SDv2-Ctrl	SDXL-Ctrl	SDv1-DR	SDv2-DR	SDXL-DR		
CNNSpot [35]	99.87	99.91	99.90	97.55	66.25	86.55	86.15	72.42	98.26	61.72	97.96	85.89	82.84	60.93	51.41	50.28	81.12	17.6
F3Net [22]	99.85	99.78	99.79	88.66	55.85	87.37	68.29	63.66	97.39	54.98	97.98	72.39	81.99	65.42	50.39	50.27	77.13	18.1
CLIP/RN50 [23]	99.00	99.99	99.96	94.61	62.08	91.43	83.57	64.40	98.97	57.43	99.74	80.69	82.03	65.83	50.67	50.47	80.05	18.3
GramNet [17]	99.40	99.01	98.84	95.30	62.63	80.68	71.19	69.32	93.05	57.02	89.97	75.55	82.68	51.23	50.01	50.08	76.62	17.0
De-fake [26]	92.10	99.53	99.51	89.65	64.02	69.24	92.00	93.93	99.13	70.89	58.98	62.34	66.66	50.12	50.16	50.00	75.52	18.4
Conv-B [19]	99.97	100.0	99.97	95.84	64.44	82.00	80.82	60.75	99.27	62.33	99.80	83.40	73.28	61.65	51.79	50.41	79.11	18.3
UnivFD [20]	98.30	96.22	96.33	93.83	91.01	93.91	86.38	85.92	90.44	88.99	90.41	81.06	89.06	51.96	51.03	50.46	83.46	17.0
DRCT [1]	94.45	94.35	94.24	95.05	95.61	95.38	94.81	94.48	91.66	95.54	93.86	93.48	93.54	84.34	83.20	67.61	91.35	4.7
Ours/DINOv2	99.55	99.55	99.55	99.54	99.55	94.70	99.53	99.23	99.31	99.55	99.54	99.55	99.39	99.48	99.55	97.42	<u>99.06</u>	<u>0.1</u>
Ours/CLIP	99.70	99.70	99.69	99.67	99.71	99.40	99.48	99.40	99.62	99.70	99.68	99.64	99.51	99.61	99.67	97.80	99.50	0.1

Table 3: Cross-dataset accuracy (Acc) performance on the Chameleon testset. All results of former methods can be sourced from the paper [36]. The first row indicates **Acc** and the second row gives **Acc on fake images/real images**.

Training Dataset	CNNSpot	FreDect	Fusing	UnivFD	DIRE	PatchCraft	NPR	AIDE	Ours/CLIP	Ours/DINOv2
SD v1.4	60.11	56.86	57.07	55.62	59.71	56.32	58.13	62.60	<u>63.94</u>	66.63
	8.86/98.63	1.37/98.57	0.00/99.96	17.65/93.50	11.86/95.67	3.07/96.35	2.43/100.00	20.33/94.38	17.27/99.01	64.65/68.12
All GenImage	60.89	57.22	57.09	60.42	57.83	55.70	57.81	65.77	<u>69.33</u>	72.07
	9.86/99.25	0.89/99.55	0.02/99.98	85.52/41.56	2.09/99.73	1.39/96.52	1.68/100.00	26.80/95.06	38.93/92.18	49.68/88.99

5 Experiments

Settings. We compare PPL to other methods across two train-test settings on three datasets:

(1) **Setting-I:** In this setting, the model is trained using real images and images from a single type of generative model. Then the models are evaluated on images from various unseen generative models. This setting assesses the detector’s cross-generator generalization ability. The datasets used in Setting-I include GenImage [47] and DRCT [1].

(2) **Setting-II:** In this setting, the model has access to a wide range of generative models during the training phase. Then the models are evaluated on a comprehensive dataset that includes challenging cases from modern generative models. Setting-II was proposed by [36] with the Chameleon dataset.

The compared methods involve basic vision models ResNet-50 [7], Conv-B[19], Swin-T [18], CNN based methods CNNSpot [35], F3Net [14], SAFE [22], CLIP based models UnivFD [20], FatFormer [16], DRCT [1], C2P-CLIP [28], AIGC detection framework Effort [37].

Implementation details. We utilized two pre-trained ViT models, CLIP [23] and DINOv2 [21], as the backbones for PPL and fine-tuned them using LoRA. For training, the input images are randomly cropped into a size of 224×224 . For testing, images exceeding 224×224 are center-cropped to this size. To achieve better performance and create paired real and fake data, we add reconstructed images with diffusion process to the training set, following the approach of DRCT [1]. To fine-tune the LORA model of CLIP or DINOv2 large with a patch-wise loss function requires 30 GB of GPU memory. Due to space limitations, additional implementation details are provided in the Appendix.

5.1 Comparison with other methods

Comparison on GenImage (Setting-I). Tab. 1 compares PPL to other methods on GenImage. We re-implement [45] and obtain the result of SAFE from [15], and the rest of the data can be sourced from C2P-CLIP[28]. We observe the following: (1) PPL consistently outperforms other methods in accuracy across various backbones. (2) The standard deviation (std) of PPL’s accuracy is significantly lower than that of the other methods, indicating greater stability across different generation methods.

Comparison on DRCT (Setting-I). Tab. 2 reports the comparison on DRCT. We obtain the results from DRCT [1]. The results indicate the following: (1) PPL consistently achieves the highest average accuracy with the lowest std. (2) DRCT shows poor detection performance on SDXL-related subsets, while PPL demonstrates a more balanced performance across various subsets. Overall comparisons in Setting-I indicate that PPL has a greater generalizing ability across different generation models.

Comparison on Chameleon (Setting-II). Fig. 3 compares the performance of PPL with other methods in the Chameleon dataset, utilizing the entire GenImage training set. Performance metrics for all the methods listed are cited from the paper [36]. The results indicate that most existing methods struggle to achieve an accuracy of approximately 55%, which only marginally exceeds the accuracy of random guessing (50%). In contrast, our method achieved an accuracy of 70% on Chameleon, surpassing the SOTA method by 5%. This demonstrates a superior generalization ability when faced with higher-quality and fine-tuned versions of generative models.

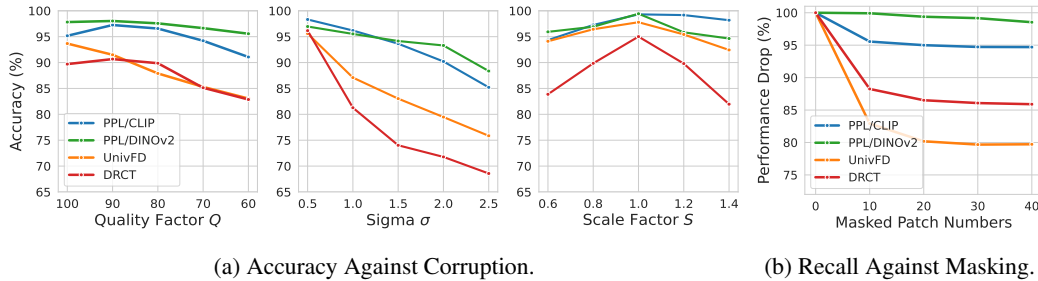


Figure 6: **(a)** Robustness to image corruptions. All methods are trained and evaluated on the SDv1.4 subset of GenImage. **(b)** Robustness to random masking. We report drop of recall rates on whole GenImage compared between the methods on masked images and the original unmasked ones.

5.2 Robustness Studies

We conduct a series of robustness experiments on GenImage to verify the reliability of our method against image corruption. Additionally, we perform robustness experiments against random masking, demonstrating PPL’s ability to leverage a greater number of available patches. For a fair comparison, we re-implemented UnivFD [20] using the same basic data augmentation (cropping, rotation, JPEG compression, etc.) as those employed in our approach.

Robustness to image corruptions. We assess the accuracy of our method under JPEG compression (quality factor $Q = 100, 90, 80, 70, 60$), Gaussian blur (standard deviation $\sigma = 0.5, 1.0, 1.5, 2.0, 2.5$) and resizing (scale $S = 0.6, 0.8, 1.0, 1.2, 1.4$) on the SDv1.4 subset of GenImage dataset. Fig. 6 illustrates that both backbones of our approach sustain high accuracy even under extreme JPEG compression and Gaussian blur, maintaining an accuracy of approximately 90%.

Robustness to random masking. We evaluate the recall rates of various methods by progressively masking portions of the input images to assess each model’s ability to detect synthetic artifacts by leveraging a greater number of patches. To account for varying initial recall values among methods, we quantify recall decline as the ratio of the decrease in recall to the original value. As shown in Fig. 6, PPL demonstrates the highest robustness against masking, with only a 5% decline under extreme masking conditions. This result confirms that PPL reduces over-reliance on specific patches.

Robustness studies demonstrate that reducing reliance on a few local patches and paying attention to patches from entire image not only improves performance metrics on academic datasets, but also enhances robustness against perturbations.

5.3 Ablation Study

To investigate the impact of each component in PPL, we conducted a series of ablation studies. Unless otherwise specified, we used CLIP as the backbone model, and trained on the SDv1.4 subset of GenImage. We then compared the overall accuracy (mACC) of each result obtained on the whole GenImage dataset.

Ablation on the impact of each module. Tab. 4 demonstrates the effectiveness of both Random Patch Replacement (RPR) and Patch-wise Contrastive Learning (PCL) on the CLIP backbone. Experimental results reveal that naive fine-tuning of a CLIP model using LoRA yields only marginal performance improvements. Furthermore, integrating RPR and PCL separately with the LoRA fine-tuning strategy leads to an increase in accuracy, proving the efficacy of both modules. Optimal performance is achieved when RPR and PCL are applied simultaneously.

Lora	RPR	PCL	mAcc (%)
			89.6
✓			91.0
✓	✓		92.6
✓		✓	92.9
✓	✓	✓	97.2

Table 4: Ablation study on each module. Models are trained on the SDv1.4 subset and tested on whole GenImage.

6 Limitations and Future Work

In this work, we note that all patches of a fully AI-generated image may contain useful synthetic artifacts and propose a patch-wise learning strategy to leverage information from all patches. Using more advanced methods and larger models to identify synthetic patches would be of our future interest and could further improve detection performance. Furthermore, with the advancement of T2I models and the growing AIGC research community, state-of-the-art models now surpass the quality of images in existing academic benchmarks. Future works would aim to build datasets close to real-world scenarios and find solutions to them, enhancing the practical utility of AIGI detection.

7 Conclusion

Our work is based on the nature of the AIGI detection problem, which can be concluded as "All Patches Matter, More Patches Better." However, our observations indicate that existing detectors are unable to fully take advantage of all patches in an AI-generated image. To address this issue, we propose a Random Patch Replacement augmentation combined with a Patch-wise Contrastive Learning strategy. This approach effectively prevents the model from becoming a lazy learner and enhances the utilization of every patch. We achieve state-of-the-art performance on several well-known academic datasets across two settings: one restricts the training set to evaluate generalization ability, while the other includes more challenging test cases without limiting the model’s training set. The outstanding performance achieved in both settings supports our findings and proves the efficacy of the proposed learning framework.

References

- [1] B. Chen, J. Zeng, J. Yang, and R. Yang. Drct: Diffusion reconstruction contrastive training towards universal detection of diffusion generated images. In *Forty-first International Conference on Machine Learning*, 2024.
- [2] J. Chen, J. Yao, and L. Niu. A single simple patch is all you need for ai-generated image detection. *arXiv preprint arXiv:2402.01123*, 2024.
- [3] D. Cozzolino, G. Poggi, M. Nießner, and L. Verdoliva. Zero-shot detection of ai-generated images. In *European Conference on Computer Vision*, pages 54–72. Springer, 2024.
- [4] S. Ghosh, K. Yu, F. Arabshahi, and K. Batmanghelich. Tackling shortcut learning in deep neural networks: An iterative approach with interpretable models. *arXiv preprint arXiv:2302.10289*, 2023.
- [5] I. J. Goodfellow et al. Generative adversarial nets. In *Advances in Neural Information Processing Systems*, 2014.
- [6] R. Hadsell, S. Chopra, and Y. LeCun. Dimensionality reduction by learning an invariant mapping. In *2006 IEEE computer society conference on computer vision and pattern recognition (CVPR’06)*, volume 2, pages 1735–1742. IEEE, 2006.
- [7] K. He et al. Deep residual learning for image recognition. In *Proceedings of the IEEE Conference on Computer Vision and Pattern Recognition*, pages 770–778, 2016.
- [8] Z. He, P.-Y. Chen, and T.-Y. Ho. Rigid: A training-free and model-agnostic framework for robust ai-generated image detection. *arXiv preprint arXiv:2405.20112*, 2024.
- [9] K. Hermann, H. Mobahi, T. FEL, and M. C. Mozer. On the foundations of shortcut learning. In *The Twelfth International Conference on Learning Representations*, 2024.
- [10] J. Ho et al. Denoising diffusion probabilistic models. *Advances in Neural Information Processing Systems*, 33:6840–6851, 2020.
- [11] T. Karras et al. Progressive growing of gans for improved quality, stability, and variation. In *International Conference on Learning Representations*, 2018.
- [12] T. Karras et al. A style-based generator architecture for generative adversarial networks. In *Proceedings of the IEEE/CVF Conference on Computer Vision and Pattern Recognition*, pages 4401–4410, 2019.
- [13] D. Konstantinidou, C. Koutlis, and S. Papadopoulos. Texturecrop: Enhancing synthetic image detection through texture-based cropping. In *Proceedings of the Winter Conference on Applications of Computer Vision*, pages 1459–1468, 2025.
- [14] J. Li et al. Frequency-aware discriminative feature learning supervised by single-center loss for face forgery detection. In *Proceedings of the IEEE/CVF Conference on Computer Vision and Pattern Recognition*, pages 6458–6467, 2021.
- [15] O. Li, J. Cai, Y. Hao, X. Jiang, Y. Hu, and F. Feng. Improving synthetic image detection towards generalization: An image transformation perspective. *arXiv preprint arXiv:2408.06741*, 2024.
- [16] H. Liu, Z. Tan, C. Tan, Y. Wei, J. Wang, and Y. Zhao. Forgery-aware adaptive transformer for generalizable synthetic image detection. In *Proceedings of the IEEE/CVF Conference on Computer Vision and Pattern Recognition*, pages 10770–10780, 2024.
- [17] Z. Liu et al. Global texture enhancement for fake face detection in the wild. In *Proceedings of the IEEE/CVF Conference on Computer Vision and Pattern Recognition*, pages 8060–8069, 2020.
- [18] Z. Liu, Y. Lin, Y. Cao, H. Hu, Y. Wei, Z. Zhang, S. Lin, and B. Guo. Swin transformer: Hierarchical vision transformer using shifted windows. In *Proceedings of the IEEE/CVF International Conference on Computer Vision*, pages 10012–10022, 2021.
- [19] Z. Liu, H. Mao, C.-Y. Wu, C. Feichtenhofer, T. Darrell, and S. Xie. A convnet for the 2020s. In *Proceedings of the IEEE/CVF conference on computer vision and pattern recognition*, pages 11976–11986, 2022.
- [20] U. Ojha et al. Towards universal fake image detectors that generalize across generative models. In *Proceedings of the IEEE/CVF Conference on Computer Vision and Pattern Recognition*, pages 24480–24489, 2023.

- [21] M. Oquab, T. Darcet, T. Moutakanni, H. Vo, M. Szafraniec, V. Khalidov, P. Fernandez, D. Haziza, F. Massa, A. El-Nouby, et al. Dinov2: Learning robust visual features without supervision. *arXiv preprint arXiv:2304.07193*, 2023.
- [22] Y. Qian et al. Thinking in frequency: Face forgery detection by mining frequency-aware clues. In *European Conference on Computer Vision*, pages 86–103. Springer, 2020.
- [23] A. Radford et al. Learning transferable visual models from natural language supervision. In *International Conference on Machine Learning*, pages 8748–8763. PMLR, 2021.
- [24] A. Ramesh, M. Pavlov, G. Goh, S. Gray, C. Voss, A. Radford, M. Chen, and I. Sutskever. Zero-shot text-to-image generation. In *Proceedings of the 38th International Conference on Machine Learning*, 2021.
- [25] R. Rombach et al. High-resolution image synthesis with latent diffusion models. In *Proceedings of the IEEE/CVF Conference on Computer Vision and Pattern Recognition*, pages 10684–10695, 2022.
- [26] Z. Sha, Z. Li, N. Yu, and Y. Zhang. De-fake: Detection and attribution of fake images generated by text-to-image generation models. In *Proceedings of the 2023 ACM SIGSAC conference on computer and communications security*, pages 3418–3432, 2023.
- [27] Z. Sun, Y. Xiao, J. Li, Y. Ji, W. Chen, and M. Zhang. Exploring and mitigating shortcut learning for generative large language models. In *Proceedings of the 2024 Joint International Conference on Computational Linguistics, Language Resources and Evaluation (LREC-COLING 2024)*, pages 6883–6893, 2024.
- [28] C. Tan, R. Tao, H. Liu, G. Gu, B. Wu, Y. Zhao, and Y. Wei. C2p-clip: Injecting category common prompt in clip to enhance generalization in deepfake detection. In *Proceedings of the AAAI Conference on Artificial Intelligence*, 2024.
- [29] C. Tan, Y. Zhao, S. Wei, G. Gu, P. Liu, and Y. Wei. Frequency-aware deepfake detection: Improving generalizability through frequency space domain learning. In *Proceedings of the AAAI Conference on Artificial Intelligence*, volume 38, pages 5052–5060, 2024.
- [30] C. Tan, Y. Zhao, S. Wei, G. Gu, P. Liu, and Y. Wei. Rethinking the up-sampling operations in cnn-based generative network for generalizable deepfake detection. In *Proceedings of the IEEE/CVF Conference on Computer Vision and Pattern Recognition*, pages 28130–28139, 2024.
- [31] R. Tang, D. Kong, L. Huang, and H. Xue. Large language models can be lazy learners: Analyze shortcuts in in-context learning. *arXiv preprint arXiv:2305.17256*, 2023.
- [32] H. Touvron, M. Cord, M. Douze, F. Massa, A. Sablayrolles, and H. Jégou. Training data-efficient image transformers & distillation through attention. In *International Conference on Machine Learning*, pages 10347–10357. PMLR, 2021.
- [33] T. J. VanderWeele. A three-way decomposition of a total effect into direct, indirect, and interactive effects. *Epidemiology*, 2013.
- [34] S. Wang, R. Veldhuis, C. Brune, and N. Strisciuglio. Frequency shortcut learning in neural networks. In *NeurIPS 2022 Workshop on Distribution Shifts: Connecting Methods and Applications*, 2022.
- [35] S.-Y. Wang et al. Cnn-generated images are surprisingly easy to spot... for now. In *Proceedings of the IEEE/CVF Conference on Computer Vision and Pattern Recognition*, pages 8695–8704, 2020.
- [36] S. Yan, O. Li, J. Cai, Y. Hao, X. Jiang, Y. Hu, and W. Xie. A sanity check for ai-generated image detection. *arXiv preprint arXiv:2406.19435*, 2024.
- [37] Z. Yan, J. Wang, Z. Wang, P. Jin, K.-Y. Zhang, S. Chen, T. Yao, S. Ding, B. Wu, and L. Yuan. Effort: Efficient orthogonal modeling for generalizable ai-generated image detection. *arXiv preprint arXiv:2411.15633*, 2024.
- [38] Z. Yan, T. Yao, S. Chen, Y. Zhao, X. Fu, J. Zhu, D. Luo, C. Wang, S. Ding, Y. Wu, et al. Df40: Toward next-generation deepfake detection. *arXiv preprint arXiv:2406.13495*, 2024.
- [39] Z. Yan, J. Ye, W. Li, Z. Huang, S. Yuan, X. He, K. Lin, J. He, C. He, and L. Yuan. Gpt-imgeval: A comprehensive benchmark for diagnosing gpt4o in image generation. *arXiv preprint arXiv:2504.02782*, 2025.
- [40] Y. Yuan, L. Zhao, K. Zhang, G. Zheng, and Q. Liu. Do llms overcome shortcut learning? an evaluation of shortcut challenges in large language models. *arXiv preprint arXiv:2410.13343*, 2024.

- [41] T. Zhang, W. Min, J. Yang, T. Liu, S. Jiang, and Y. Rui. What if we could not see? counterfactual analysis for egocentric action anticipation. In *IJCAI*, pages 1316–1322, 2021.
- [42] X. Zhang et al. Detecting and simulating artifacts in gan fake images. In *2019 IEEE International Workshop on Information Forensics and Security (WIFS)*, pages 1–6. IEEE, 2019.
- [43] Y. Zhang, Y. Wei, D. Jiang, X. Zhang, W. Zuo, and Q. Tian. Controlvideo: Training-free controllable text-to-video generation. *arXiv preprint arXiv:2305.13077*, 2023.
- [44] L. Zhao, Q. Liu, L. Yue, W. Chen, L. Chen, R. Sun, and C. Song. Comi: Correct and mitigate shortcut learning behavior in deep neural networks. In *Proceedings of the 47th International ACM SIGIR Conference on Research and Development in Information Retrieval*, pages 218–228, 2024.
- [45] C. Zheng, C. Lin, Z. Zhao, H. Wang, X. Guo, S. Liu, and C. Shen. Breaking semantic artifacts for generalized ai-generated image detection. In *Advances in Neural Information Processing Systems*, 2024.
- [46] N. Zhong, Y. Xu, S. Li, Z. Qian, and X. Zhang. Patchcraft: Exploring texture patch for efficient ai-generated image detection. *arXiv preprint arXiv:2311.12397*, pages 1–18, 2024.
- [47] M. Zhu, H. Chen, Q. Yan, X. Huang, G. Lin, W. Li, Z. Tu, H. Hu, J. Hu, and Y. Wang. Genimage: A million-scale benchmark for detecting ai-generated image. *Advances in Neural Information Processing Systems*, 36, 2024.